New constraints on the black-hole candidate XTE J1908+094 from the Swift/XRT spectral data

Xavier Fernández-Real Girona and Gerard Neras Lozano
Universitat Politècnica de Catalunya - BarcelonaTech
ETSETB, Enginyeria Física
(Dated: May 28, 2014)

We present the X-ray light curves and the corresponding spectral analysis of XTE J1908+094 using the *Swift* Gamma-Ray Burst Mission recent observations, covering an outburst from November 2013. Assuming that the Eddington's limit is attained and by fitting the data with a black body disk model to the observed spectrum at maximum flux we deduced the mass of the compact object of the binary system with respect to the distance and inclination of the disk: $M/M_\odot = (0.5 \pm 0.1)d_{10}^2(\cos\theta)^{-1}$ (d_{10} in units of 10 kpc). Moreover, the inner temperature obtained of $T_{in} = 0.75 \pm 0.02$ keV is a clear evidence that the identity of the object is a black-hole, thus allowing us to represent a region of possible distances and inclinations, which is consistent with other works that indicate a high inclination.

I. INTRODUCTION TO BLACK HOLES AND X-RAYS

A. General description

In terms of thermodynamics, black holes are considered perfect black bodies, i.e., objects that absorb all light without reflecting any part of it. The usual understanding of a black hole is a region of space bounded by a surface called *event horizon*, defined as the set of points from where light cannot escape. The *event horizon* is considered to be a sphere of a certain critical radius called Schwarzchild radius, which is found to be $R_S = 2GM/c^2$ according to general relativity (in terms of M mass of the object).

There are essentially two kinds of black holes that can be detected: supermassive black holes (found in the center of most galaxies), which are black holes that have absorbed other stars or have merged with other black holes; and black holes in X-ray binaries.

X-ray binaries are binary stars that emit X-ray light. They are formed by a normal star and a compact object, specifically a neutron star or a black hole. The first object acts as a *donor* while the compact object is the *accretor*.

At some point of the evolution of the donor, it may expand past its Roche lobe (region of space around the donor where mass is kept gravitationally bound to it). A transfer of matter from the donor to the accretor will occur. The accreted mass can either fall into the compact object or it can form a disk of matter around it called accretion disk. If the latter occurs (which will be always, unless there are strong magnetic fields), the inner part of the accretion disk will eventually fall into the accretor as well. When this mass is absorbed, it loses a considerable part of its energy as radiation, which given the conditions of the system will be emitted as X-rays (the temperature in the accretion disk is such that the peak of radiation is found in the X-ray part of the spectrum, due to viscous stresses heating the material to millions of degrees, which helps the disk to lose the angular momentum and eventually fall). This emission is called an *outburst*, and it produces a peak in the light curve of the object. When an X-ray binary has reached the point where outbursts occur, it is said to be a *transient source*.

Black holes can be identified by their mass. When a star collapses after nuclear fusion reactions have ended, the mass of the resulting compact object is determined by the mass of the progenitor star, black-holes originating from star more massive than $\sim 10M_\odot$. The limit between the mass of the final neutron star and a black hole is believed to be around $3M_\odot$ (solar masses), where black holes are the most massive.

In this project, in order to identify a black hole candidate, its X-ray light curve is observed during its outburst. The light curve is the representation of the light intensity of the X-ray binary as a function of time. When an outburst occurs, the light curve rises and falls again during a period of some weeks. The peak of the light curve during the outburst gives the most significant information about the black hole candidate, because it is possible to assume, as an approximation, that this peak occurs in the Eddington's limit. Therefore, one can extract the mass of the object.

B. Eddington's limit

The Eddington's limit, also known as Eddington's luminosity, refers to the maximum luminosity a star or a galaxy can emit in order to have an equilibrium between the gravitational force of the body (towards its center) and the radiation force produced by this luminosity (towards the outside of the object, opposite to the center). Beyond this limit, the radiation pressure overcomes gravity and therefore the material in the surroundings of the object will be forced away, rather than being attracted by it.

The derivation of the limit is rather easy to obtain, making some assumptions regarding the influence of the gravitational force and the photons on the protons and electrons, thus yielding the following expression:

$$L_{edd} = \frac{4\pi G M c m_p}{\sigma_T} = 1.26 \cdot 10^{38} \left(\frac{M}{M_\odot}\right) erg/s \qquad (1)$$

Where $M_\odot$ is the mass of the Sun, σ_T is the Thompson scattering cross-section for the electrons, m_p is the mass of the proton and M is the mass of the object considered.

C. The soft-state of black-hole binaries

X-ray binaries show several different contributions to the X-ray spectrum. In general, the X-ray spectrum of X-ray binaries has a soft X-ray component of thermal origin, and a hard X-ray emission explained by Compton scattering in a hot corona. Depending on the total luminosity and contribution of these components to the X-ray spectrum, it is possible to classify it as particular spectral states. Black-hole binaries can display transitions between the different states.

The most important classification of states refers to two different possibilities: high/soft state and low/hard state. In the former case, the emission is basically dominated by the thermal part, and it is the situation on which this essay will focus.

The soft-state or thermal state of the X-ray binary systems is dominated by the thermal radiation from the inner parts of the accretion disk. This kind of X-ray energy spectrum can be modeled by an accretion disk model, radiating as a multi-temperature black-body [6]. In a more accurate perspective, the model is based in the thin disk model by Shakura and Sunyaev [7], where the temperature profile of the disk has an inverse relation with the radius.

Although this rather simple model achieves good results, in order to obtain a higher accuracy it is needed to consider more realistic inner boundary conditions, a general relativity view of the gravitational potential rather than just the Newtonian one, Thomson scattering, Doppler effect due to rotation and quite a lot of other effects. Many models considering some of this features are already implemented in the XSPEC package, introduced below.

II. INSTRUMENTATION

A. Swift Gamma-Ray Burst Mission

The Swift Gamma-Ray Burst Mission was launched into orbit on November 20, 2004, and is managed by the NASA Goddard Space Flight Center. *Swift* has three different instruments, the BAT (Burst Alert Telescope), the XRT (X-ray Telescope) and the UVOT (Ultraviolet/Optical Telescope).

The XRT is the X-ray telescope in the *Swift* spacecraft in charge of taking images and performing spectrography in the X-ray band, 0.1-10 keV. It can cover up to seven orders of magnitude in flux and has a pixel scale of 2.36 arc-seconds per pixel, reaching an accuracy of just 5 arc-seconds within 10 seconds of target acquisition. The XRT uses a JET-X Walter I telescope focused onto a MOS charged-coupled device CCD-22, with an image area of 600×602 pixels ($40\ \mu$m $\times$ 40μm). It has a sensitivity limit of $2 \cdot 10^{-14}$erg$\cdot$cm$^{-2}\cdot$s^{-1} or $2 \cdot 10^{-17}$J$\cdot$m$^{-2}\cdot$s^{-1} in 10^4 seconds.

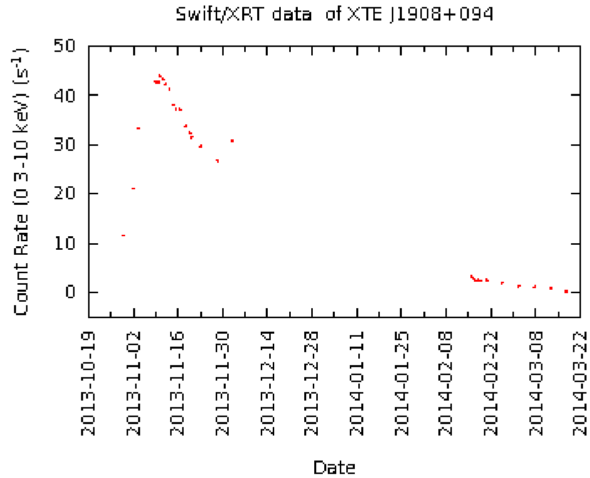

Figure 1. Swift-XRT light curve of XTE J1908+094 by date

III. SWIFT DATA PRODUCTS AND SPECTRAL ANALYSIS

A. Data products

The main data products used in X-ray astronomy are event lists. Event lists contain lists of parameters associated to events (i.e., photons) observed by an instrument, where these parameters registered are position, time and energy of the photons. By accumulating histograms of events' parameters it is possible to build images, light curves and spectra.

B. Spectral analysis

The data products derived from the Swift observations need to be treated in order to compare them with physical models. In this project we deal with the spectral fitting, done with XSPEC, and X-ray spectral fitting package[1].

The spectrum directly obtained from the data does not correspond to a particular physical model, but instead it contains deviations due to different factors. First of all, the spectrometer does not obtain directly the observed spectrum but photon counts. The detection device has a probability to detect photons of each energy through different channels, and therefore the received spectrum is actually weighted according to some function, that depends on the channel and the energy of the incoming photons. In order to fit a spectral model, it is necessary to invert this process, which is non-trivial and most of the times impossible (due to the non injectivity or the low stability of this process). Instead of reverting the effect of the instrument on the data, XSPEC folds the instrument response to the theoretical model and compares that with the data. The best-fit parameters of the model are determined by minimization of χ^2. Through

[1] http://heasarc.gsfc.nasa.gov/docs/software/lheasoft/

this process, it is taken into account the instrumental response against a particular spectral model.

Apart from that, it is also necessary to correct the source spectrum from the background. In general, in order to perform a spectral fitting through XSPEC it is necessary to have the spectrum, the effective area, the response matrix (specific of each instrument) and the background spectrum.

IV. SWIFT-XRT LIGHT CURVE OF XTE J1908+094

The light curve of XTE J1908+094 by date can be found in Figure 1, whose data has been extracted from the *Swift* website[2]. There are only represented the dates in which there are observations from the last months. A peak is registered at an observation with date 2013-11-10 05:29 UTC. The main shape of the graph corresponds to the characteristic function of this kind of outburst, where the rise has a higher slope in absolute value than the subsequent decrease.

Before proceeding to the spectral analysis, we check that the flux during the chosen observations is approximately constant. For our project, we consider the higher luminosity data, the ones with higher count rate, so that it can afterwards be compared to the Eddington's limit.

According to the previous figure presented, there are some observations near the peak value. In this case, the main four observations are going to be considered, the four with higher count rate (over 40 s^{-1}). In order to check the variability of the observations considered, the light curve must be plotted. It is also necessary to check the variability of the background to rule out high count rate periods due to other contributions rather than the observed object itself.

In all four cases it has been checked that the background effect is negligible and constant with time (no unusual successes are stored as information). Moreover, the hardness ratio is also approximately constant, which indicates a certain degree of confidence in the validity of the spectrum detected. As a general approach, the hardness ratio indicates the ratio between hard (1.5-10 keV) and soft (0.3-1.5 keV) photons in the X-ray part of the spectrum detected by the telescope; i.e., a constant hardness ratio is a characteristic of a constant spectrum, with no significant deviations.

V. PREVIOUS OBSERVATIONS

The object, XTE J1908+094, has been previously observed and analysed with no significant results regarding its identity. It has been possible to study its optical, IR and radio counterparts and obtain rather significant results during the periods of low emission of the black-hole candidate: [10] and [11]. On the other hand, some studies have found evidences towards the idea of the compact object being a black-hole, all based on the analysis of the spectrum (specially the hard spectrum) and comparing the results obtained to other known black-holes, [12, 13]. However, none of them obtains a significant result, and therefore it has not been yet proved whether XTE J1908+094 is a black-hole binary or not.

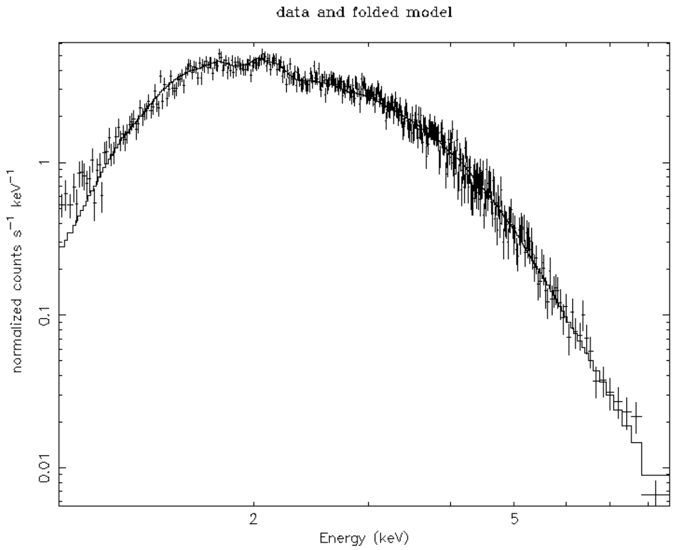

Figure 2. Spectrum of the observations for energies higher than 1 keV.

VI. RESULTS

Putting the main four observations together it is possible to begin with the spectral analysis. One of the first steps is to check whether the observations present *pile-up* (photons' flux too high in some regions), and to try to avoid this possible error we treated directly with level 1 data. From this point it is possible to select the observation region (excluding the brightest zone) and the background region manually, through SAOImage DS9 [3]. Thus, it is only considered the most reliable data. Apart from that, it is generated an *arf* file consisting of the information of the telescope response, and a *rmf* file of the detector response.

The spectrum is fitted through a soft black body model (*diskbb* model of XSPEC, [6, 14]), together with an interstellar absorption model, *TBabs* [15]. These models use abundances of elements and cross-sections from predefined tables not necessary updated. For this project, the tables used are changed to *wilm* tables for the abundances, [15], and *vern* for the cross-sections, [16].

When performing the first fit, the model does not fit appropriately the high and low energies (χ^2 is larger than 8). In order to correct the high energies fitting we add a *power law* model, which leads to an improve in χ^2. This power law is added to correct the inverse Compton effect that appears due to a high temperature cloud of

[2] http://www.swift.ac.uk/user_objects/

[3] http://ds9.si.edu/

electrons known as corona. Through this procedure the reduced χ^2 decreases to around 7, still a bad value due to a bad fitting for low energies. The reason of the bad fitting is unknown, although it might be related to the scattering of photons of low energy in the dust around the compact object. To avoid treating with a model obtaining conclusions from a bad fitting, the low energies are ignored, and we only consider energies higher than 1 keV (yielding, thus, a reduced χ^2 of just 1.097). The fitted model together with the data is presented in Figure 2.

Using the previous three models introduced, the absorption model is fitted with a value for nH (hydrogen column density) of $3.66 \cdot 10^{-22}\mathrm{cm}^{-2}$, whereas the average interstellar hydrogen column density in this direction is of $1.50 \cdot 10^{-22}\mathrm{cm}^{-2}$ [17]. A value higher than the interstellar one might indicate a poor fit, the presence of circumstellar matter increasing the absorption column or a high distance. In this situation we assume it is an evidence of a distance larger than the typical interstellar of 1-2 kpc, the distance to the interstellar gas slab responsible for the average interstellar hydrogen column density. We assume the distance to be between 5 and 10 kpc. It is possible to fit the models fixing previously the hydrogen column density to $1.5 - 2.5 \cdot 10^{-22}\mathrm{cm}^{-2}$, but the fitting is even worse, reaching values for χ^2 up to 3.6.

For this project, we are interested in the values of T_{in}, indicating the inner temperature of the disk, and $norm$, which gives the value of $((R_{in}/km)/(D/10kpc))^2 \cos\theta$, where R_{in} is the inner radius of the disk, D is the distance to the object (in units of 10 kpc), and $\cos\theta$ is the correction added due to the inclination of the disk with respect to the normal plane as seen from the Earth.

Performing the fitting of the model with variations in the parameters $norm$ and T_{in}, it is possible to obtain a region of values with confidence 1-σ according to the χ^2 test. The parameters are found to be $norm = 1500 \pm 200$ and $T_{in} = 0.75 \pm 0.02$ keV, considering the outer parts of the contour of confidence 1-σ. This low value for the inner temperature is a clear indication of a black-hole. This is because the inner part of the disk is always the hotter, and in a black-hole the inner part is absorbed by the black-hole itself, whereas in a neutron star the accretion disk can be located up to the surface of the star.

It is possible to obtain a lower limit for the mass of the object, through the Eddington's limit. The luminosity can be known through the approximation: $L_{dbb} = 4\pi R_{in}^2 \sigma T_{in}^4$ (σ represents here the Stefan–Boltzmann constant). For this situation it is obtained $L_{dbb} = (6 \pm 1) \cdot 10^{37} d_{10}^2 (\cos\theta)^{-1}$ erg s^{-1}, where d_{10} represents the distance to the object, expressed in units of 10 kpc. Comparing this result to the Eddington's limit, it is obtained the mass of the object in solar masses:

$$\frac{M}{M_\odot} = (0.5 \pm 0.1) d_{10}^2 (\cos\theta)^{-1} \quad (2)$$

At this point, one could think that for most of the possible distances and inclinations the object shows a mass lower than 3 solar masses, and therefore the object could be considered a neutron star. However, for the particular case of XTE J1908+094, previous works show that the system is observed at a high inclination, with an angle between the disk rotation axis and the observer's view between 86.2 and 90 deg in [13] (i.e., the system is observed almost edge-on). This results in $M/M_\odot > 7.2 d_{10}^2$. Thus, assuming a distance of at least 7 kpc, the mass obtained is more than 3 solar masses, which indicates a black hole. In the Figure 3 it is presented a graph where the mass is represented as a function of the inclination and distance.

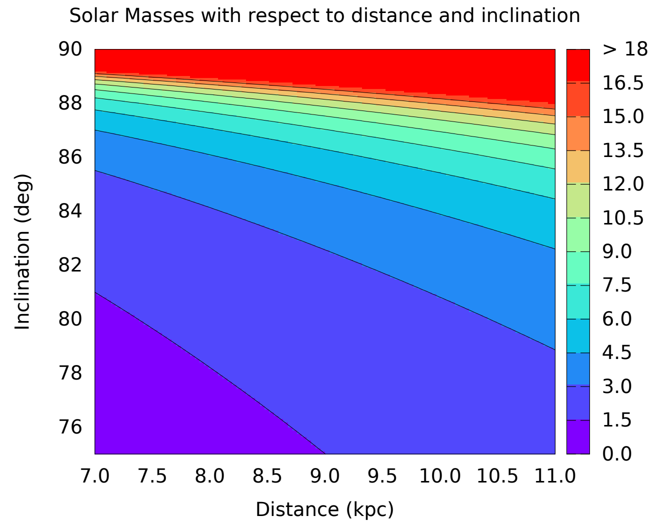

Figure 3. Mass of the object as a function of distance and inclination as seen in equation (2). The second line from below represents the points at which the mass of the object would be exactly 3 solar masses. Any point above this line would lead to deduce that the compact object is a black-hole.

This result can also be used the other way round. Since the inner temperature of the disk shows that the object is most likely a black-hole (if it was a neutron star, this temperature would reach values between 2 and 3 keV), and assuming that this kind of black-holes usually have a mass lower than 5 solar masses; the distance to the object is found to be at most 8.3 kpc.

Repeating the procedure changing the model used to *diskpn* [18], an extension of the previous model that includes corrections for temperature distribution near the black-hole, it is obtained a value for the mass of the object of $\frac{M}{M_\odot} = (4.8 \pm 0.9) d_{10} (\cos\theta)^{-1/2}$. The reduced χ^2 for this model is slightly worse than the previous one, of 1.1112, without a significant difference. This model deals with one parameter not present in *diskbb*, β, which is the color/effective temperature ratio, and has been taken to be $\beta = 1.7 \pm 0.1$. Moreover, it has also been obtained the parameter T_{max}, analogous to the previous T_{in}, which is $T_{max} = 0.71 \pm 0.03$keV, similar to the temperature from *diskbb*. The fact that the temperature again is low, gives more credit to the hypothesis of the object being a black-hole.

VII. CONCLUSIONS

The mass of the object studied has been found to be $M/M_\odot = (0.5 \pm 0.1) d_{10}^2 (\cos\theta)^{-1}$, which gives a value higher than 3 taking into account that other papers suggest a high inclination and a rather large distance (higher than 5 kpc), [10, 11, 13]. This fact, together with a rather low inner temperature of $T_{in} = 0.75 \pm 0.02$ keV both suggest that XTE J1908+094 is a black-hole, supporting the idea of other researchers who already studied the object. From this point, it is possible to get an upper bound for the distance to the binary system of 8.3 kpc, which can be improved if the inclination of the disk is determined more accurately. A similar conclusion can be reached through the analysis of the data using the *diskpn* model instead of the *diskbb*, which adds corrections to the latter model.

Bounding the mass of the object between 3 and 4 solar masses, it is also possible to obtain a relation between the inclination and the distance to the object. Since the inclination can be determined by means of radio emission studies, through this result it will be possible to get the distance to the binary system as a function of the inclination, $d_{10} = (2.7 \pm 0.5) \cos^{1/2}\theta$ setting the mass $M/M_\odot = 3.5 \pm 0.5$. For example, for an inclination of 88 deg, this expression would lead to a distance of 5.0 ± 0.8 kpc.

VIII. ACKNOWLEDGEMENTS

This project has been possible thanks to the guidance of Glòria Sala, who spent many hours in order to help us reach a conclusion.

[1] *The Swift Gamma-Ray Burst Mission*, National Aeronautics and Space Administration (NASA), 30 July 2013 Web. 20 Apr. 2014 `http://swift.gsfc.nasa.gov/`.
[2] *Overview of the Swift X-ray Telescope*, Pennsylvania State University (PSU), Web. 20 Apr. 2014 `https://www.swift.psu.edu/xrt/`.
[3] *Swift's X-Ray Telescope (XRT)*, National Aeronautics and Space Administration (NASA), 14 Feb. 2012 Web. 20 Apr. 2014 `http://swift.gsfc.nasa.gov/about_swift/xrt_desc.html`.
[4] Cucchiara, A. et al (2011), ApJ, 736, 12.
[5] Karttunen, H. et al, *Fundamental Astronomy*, Fifth edition, Springer, 2007.
[6] Makishima, K. et al (1986), ApJ, 308, 635-643.
[7] Shakura, N. I.; Sunyaev, R. A. (1973), A&A, 24, 337-355.
[8] Wei, D. *X-Ray Power Density Spectra of Black Hole Binaries: A New Deadtime Model for the RXTEPCA*, Massachussetts Institute of Technology (MIT), June 2006 Web. 5 Apr. 2014. `http://heasarc.gsfc.nasa.gov/docs/xte/pca/dwei_thesis.pdf`
[9] Titarchuk, L.; Shaposhnikov, N. (2005), ApJ, 626, 298-306.
[10] Chaty, S. et al (2002), ApJ, 337, L23-L26.
[11] Chaty, S. et al (2006), Mon. Not. R. Astron. Soc., 365, 1387-1391.
[12] Göğüş, E. et al (2004), ApJ, 609, 977-987.
[13] Zand, J.J.M. et al (2002), A&A, 394, 553-560.
[14] Mitsuda et al. (1984), PASJ, 36, 741.
[15] Wilms, Allen and McCray (2000), ApJ 542, 914-924.
[16] Verner, D.A. et al. (1996), ApJ, 465, 487.
[17] Kalberla, P. M. W. et al. (2005), A&A, 440, 775-782.
[18] Gierlinski, M. et al. (1999), MNRAS, 309, 496-512.